# Voltage-controlled group velocity of edge magnetoplasmon in the quantum Hall regime

H. Kamata,[1,2] T. Ota,[1] K. Muraki,[1] and T. Fujisawa[2]

[1]*NTT Basic Research Laboratories, NTT Corporation, 3-1 Morinosato-Wakamiya, Atsugi, Kanagawa 243-0198, Japan*
[2]*Research Center for Low-Temperature Physics, Tokyo Institute of Technology, 2-12-1 Ookayama, Meguro, Tokyo 152-8551, Japan*

We investigate the group velocity of edge magnetoplasmons (EMPs) in the quantum Hall regime by means of time-of-flight measurement. The EMPs are injected from an Ohmic contact by applying a voltage pulse, and detected at a quantum point contact by applying another voltage pulse to its gate. We find that the group velocity of the EMPs traveling along the edge channel defined by a metallic gate electrode strongly depends on the voltage applied to the gate. The observed variation of the velocity can be understood to reflect the degree of screening caused by the metallic gate, which damps the in-plane electric field and, hence, reduces the velocity. The degree of screening can be controlled by changing the distance between the gate and the edge channel with the gate voltage.

PACS number(s): 73.43.Lp, 73.43.Fj, 73.50.Mx

## I. INTRODUCTION

When a strong magnetic field is applied perpendicular to the two-dimensional electron gas (2DEG), electrons propagate in one-dimensional edge channels, which form along the edge of the sample in the quantum Hall regime.[1] Recently, edge channels have attracted much attention as a coherent one-dimensional channel without dissipation. For example, electronic Hanbury Brown-Twiss,[2] Mach-Zehnder,[3] and Fabry-Pérot[4–6] interferometers have been realized experimentally by employing edge channels together with quantum point contacts (QPCs) to split and join them. These interferometric experiments allow us to study coherent transport and quantum statistics of electrons.[7–9] On the other hand, a single-electron source has been realized by tailoring the time-dependent electrochemical potential of a quantum dot connected to an edge channel.[10] These experiments motivate the study of electronic quantum channels, which carry quantum states over a long distance extending over the whole device. For such purposes, the electron velocity is one of the important characteristics to control the timing of the transmission.[11]

When nonequilibrium excess charge is induced in the edge channel, for example, by applying a voltage pulse or microwave, the charge propagates along the edge of the sample in the form of an edge magnetoplasmon (EMP). EMPs have been widely investigated both theoretically[12–15] and experimentally.[16–18] For example, high-frequency magnetoconductivity measurements and time-of-flight experiments have shown that the group velocity of the EMPs is inversely proportional to the magnetic field $B$.[16–18] The reported velocity of the EMPs is $1000 \sim 1500$ km/s at bulk filling factor $\nu = 2$ when the edge channel is formed along a chemically etched mesa structure.[16,17] On the other hand, a much smaller velocity ($\sim 150$ km/s at $\nu = 2$) was observed when the surface of the structure was covered by a metal.[18] Although the difference is believed to be due to image charge or screening by the surface metal,[15] no systematic study has been carried out in the intermediate region.

In this paper, we investigate the group velocity of EMPs traveling along the edge channel defined by a semi-infinite metallic gate. We find that the group velocity strongly depends on the gate voltage (280–430 km/s at $\nu = 2$). The observed gate voltage dependence can be qualitatively understood by considering the degree of screening. The electrically tunable group velocity is attractive for controlling the timing of EMP transport.

## II. TIME-OF-FLIGHT MEASUREMENT WITH A QUANTUM POINT CONTACT

In previous measurements of EMPs in the frequency or time domains, EMPs were detected with relatively large Ohmic contacts[17,18] or gate electrodes.[16] Here, we use a QPC as a local probe of the charge or the associated potential created by EMPs. This experimental technique was originally developed for evaluating time-dependent potentials induced by external voltage pulses.[19] In this paper, we utilize this technique to study charge dynamics of EMPs.

Figure 1(a) schematically shows the device structure and experimental setup. The structure, fabricated on an AlGaAs/GaAs modulation-doped heterostructure, consists of a QPC defined by a standard split-gate technique and four additional metallic gates serving as "delay gates" to tune the path length (used in Sec. III). The 2DEG located 110 nm below the surface has a density of $3.2 \times 10^{15}$ m$^{-2}$ and a low-temperature mobility of 170 m$^2$/Vs. The following measurements were performed in a dilution refrigerator at about 50 mK. A constant magnetic field of $B = 6.5$ T was applied to the 2DEG, which corresponds to a bulk filling factor $\nu = 2$.

When a voltage pulse, $V_{PS}(t)$, is applied to the source Ohmic contact, a pulse of EMPs is generated and then travels chirally along the edge channel as schematically shown in Fig. 1(a). The charge in the form of the EMP pulse occupies the Landau Levels up to the electrochemical potential $\mu(\xi, t)$, which depends on the distance ($\xi$) along the edge channel from the source. Figure 2(a) schematically shows the potential $\mu(\xi, t)$ around the QPC for a single Landau level, with the formation of a compressible strip neglected. If the dispersion of the EMP pulse is approximated to be a linear function with a constant velocity $v$, the dynamical potential can be written in the simple form $\mu(\xi, t) = \mu'(t - \xi/v)$. Then,
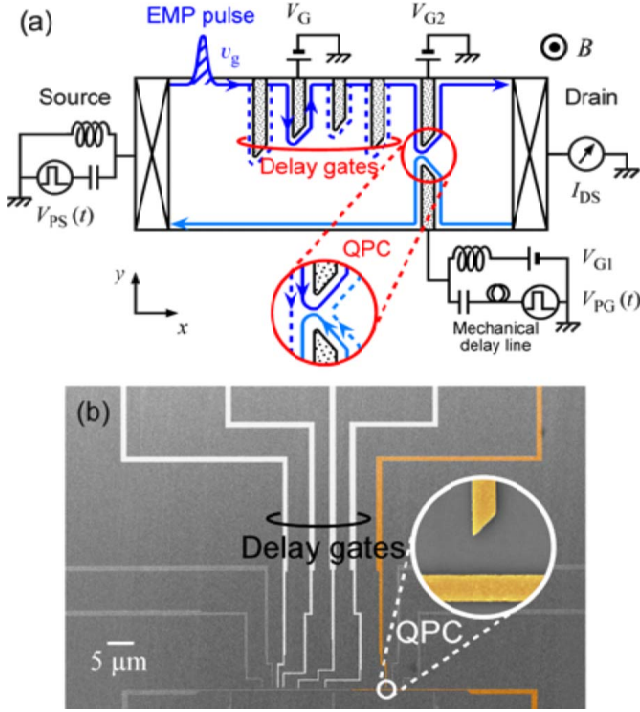
FIG. 1. (Color online) (a) Schematic device structure and experimental setup for time-of-flight measurement. A short voltage pulse $V_{PS}(t)$ of 1.0 mV in amplitude is applied to the source to inject a pulse of EMPs. Another voltage pulse $V_{PG}(t)$ of 20 mV in amplitude is applied to the QPC to probe the local potential. The time interval between the two voltage pulses is changed by the mechanical delay line. Four delay gates between the source and the QPC can be used to add extra path length. (b) A scanning electron micrograph of the device. The white lines are metallic gates for the delay gates. The QPC is shown in an enlarged view inside the white circle. Disabled gates are biased at $\sim +0.2$ V to minimize backscattering. The complicated gate patterns are designed for another purpose, but their different perimeters are useful for this work.

the potential arrives at the QPC (at a distance $\xi_Q$) with a delay time of $\xi_Q/v$ after the application of the voltage pulse to the source. Another voltage pulse, $V_{PG}(t-t_d)$, is applied to the lower gate of the QPC in the tunneling regime to probe the local potential. Here, $t_d$ is the time interval between the two voltage pulses, which can be experimentally controlled with a mechanical delay line and a pulse pattern generator as shown in Fig. 2(b). The pulse applied to the QPC changes the barrier potential of the QPC, $U(t)$, and hence the conductance, $G_Q(t)$, by $\Delta G_Q(t) \propto \Delta U(t) \propto V_{PG}(t)$ for sufficiently small amplitude of the pulse. In the linear transport regime, the current through the QPC, $i(t)$, is proportional to the potential difference $\Delta \mu(t) = \mu(\xi_Q, t) - \mu_D$ across the QPC, where $\mu_D$ is the (time independent) electrochemical potential of the drain. Instead of measuring $i(t)$ directly, we measured the average current $I_{DS}(t_d) = \langle i(t) \rangle$ as a function of $t_d$. Then, the average current has a form of correlation function,

$$I_{DS}(t_d) = \frac{1}{e} \langle \Delta G_Q(t-t_d) \Delta \mu(t) \rangle. \tag{1}$$

One can evaluate the time-dependent local potential $\Delta \mu(t)$ if $\Delta G_Q(t)$ abruptly changes in a delta-function $\Delta G_Q(t) \propto \delta(t)$ or
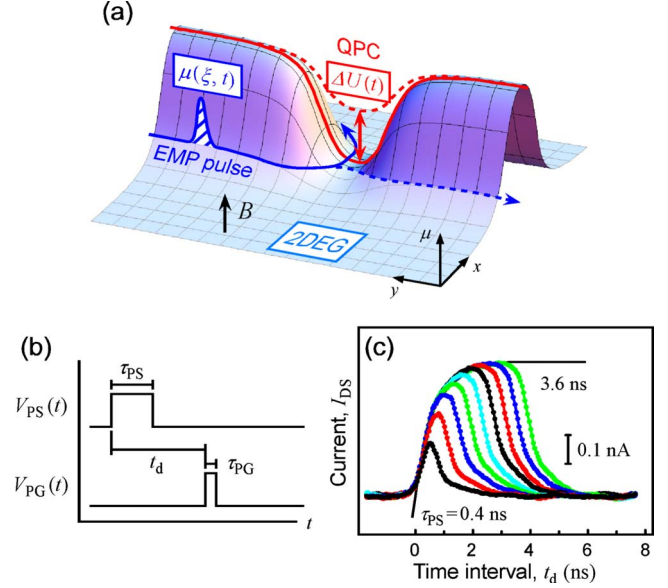


FIG. 2. (Color online) (a) Schematic potential diagram of the EMP pulse and the QPC. If the timing of the voltage pulse applied to the QPC coincides with the arrival of the EMP pulse at the QPC, the EMP pulse passes through the QPC (solid line); otherwise, the EMP pulse is reflected at the QPC and returns to the source contact (dashed line). (b) Schematic pulse patterns of the two voltage pulses. (c) $I_{DS}(t_d)$ curves observed at $B=6.5$ T for various pulse widths. The solid line is an exponential fit.

in any known functions. The actual potential waveforms in the device can be estimated by analyzing $I_{DS}(t_d)$ for various pulse widths.[19]

The $I_{DS}(t_d)$ curves shown in Fig. 2(c) were obtained by varying the pulse width $\tau_{PS}$ of $V_{PS}(t)$ from 0.4 to 3.6 ns while keeping the pulse width $\tau_{PG}$ of $V_{PG}(t)$ constant at 0.08 ns (minimum available pulse width in our setup). The peak width in the observed $I_{DS}(t_d)$ curve increases with pulse width $\tau_{PS}$. Since $\Delta G_Q(t)$ effectively changes in a delta function, the observed $I_{DS}(t_d)$ curves reflect the time evolution of the EMP pulse in the device. Here, the time constant of 0.6 ns, which is obtained by fitting with an exponential function [Fig. 2(c), solid line] is larger than that measured at zero magnetic field (0.28 ns).[19] The increased time constant may be related to the higher Ohmic resistance in the magnetic field or to the nonlinear dispersion of EMPs, which will be investigated in the future. In this way, we can evaluate the time-dependent potential or the charge distribution of the EMP pulse. In this paper, we focus on the velocity of the EMPs. The following data were measured at $\tau_{PS}=0.4$ ns and $\tau_{PG}=0.08$ ns.

## III. EXPERIMENTAL RESULTS

Edge channels can be defined either by chemically etching the heterostructure or electrostatically depleting the 2DEG under a metallic gate. Edge channels defined by a metallic gate are useful for electrical switching of the path length. Here, we use four additional gates (delay gates; typically $\sim 100$ $\mu$m in length) between the source contact and
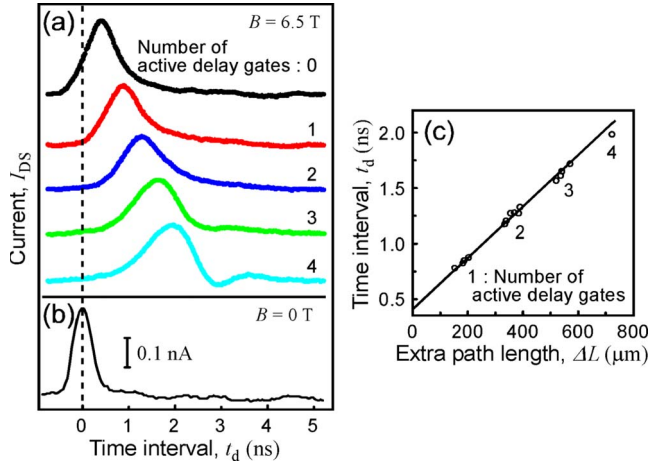
FIG. 3. (Color online) (a) and (b) $I_{DS}(t_d)$ curves observed at (a) $B=6.5$ T ($\nu=2$) and (b) $B=0$ T. The origin of the time interval is chosen at the peak position of the reference data in (b). Active delay gates are biased at $V_G=-1.1$ V. These curves are offset for clarity. (c) Time interval for various extra path length $\Delta L$ with a straight-line fit.

the QPC [Fig. 1(b)], which add extra path length (the perimeter), $\Delta L$, by depleting electrons underneath with a negative gate voltage $V_G$ (below the pinch-off voltage of $\sim-0.2$ V). Since these gates are slightly different in perimeter, we can choose 16 kinds of path lengths by combining them.

The top curve in Fig. 3(a) shows the $I_{DS}(t_d)$ observed at $B=6.5$ T ($\nu=2$) when no delay gates are activated (the number of the active delay gate is 0). As compared with the reference data observed at zero magnetic field [Fig. 3(b)], the curves observed at $B=6.5$ T [Fig. 3(a)] is significantly delayed. When no delay gates are activated, the EMP pulse injected from the source travels along the chemically etched edge ($\sim400$ $\mu$m in length) and the edge defined by a metallic gate (the upper gate of the QPC; $\sim100$ $\mu$m in length) until it reaches the QPC detector. The observed delay time of $t_d\sim0.5$ ns corresponds to the mean group velocity of $\sim1000$ km/s, which is consistent with the previous reports.[16,17]

As the number of active delay gates ($V_G=-1.1$ V) and hence the extra path length $\Delta L$ is increased, the delay of the EMP pulse increases as shown in Fig. 3(a). The delay time $t_d$ is proportional to $\Delta L$ as shown in Fig. 3(c). From the slope, the group velocity of the EMP pulse traveling along the delay gates can be precisely determined to be $v_g=430$ km/s at $V_G=-1.1$ V. The obtained velocity is smaller than the reported value in the unscreened case[16,17] but larger than that in the high-screening case.[18]

We find that the velocity strongly depends on the gate voltage $V_G$. Figure 4(a) shows the variation of $I_{DS}(t_d)$ observed when only one of the delay gates ($\Delta L=205$ $\mu$m) is activated at different $V_G$. The peak position indicated by the arrows shifts with $V_G$. By measuring the $\Delta L$ dependence of $t_d$ at various $V_G$, we obtain the velocity as a function of $V_G$ as shown in Fig. 4(b). As $V_G$ is made more negative, the depletion region spreads as illustrated in Fig. 4(c) and, hence, the edge channel is pushed further away from the metallic gate. Therefore, the observed variation of $v_g$ is considered to re-
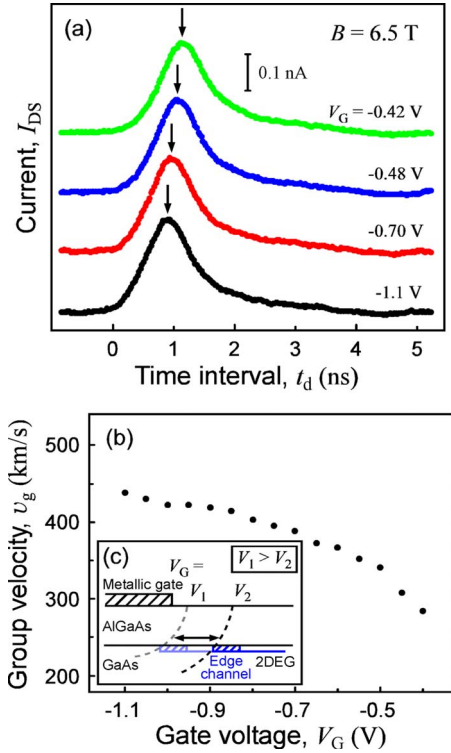


FIG. 4. (Color online) (a) $I_{DS}(t_d)$ curves observed for various $V_G$. These curves are offset for clarity. (b) Group velocity $v_g$ as a function of $V_G$. (c) Schematic cross-section of the heterostructure. The location of the edge channel is shifted away from the gate as the 2DEG is depleted.

flect the degree of screening by the metallic gate.

Here, several points need to be addressed. First, we note that the path length slightly changes with $V_G$ since the distance between the edge channel and the gate changes with $V_G$. However, the change (estimated to be a few 100 nm) is negligibly small as compared with the total path length (a few 100 $\mu$m). Moreover, the path length increases as $V_G$ is made more negative, which does not account for the earlier arrival of the EMP pulse. Second, the delay gates have complicated shapes with varying widths (0.1$\sim$1 $\mu$m) and corners as shown in Fig. 1(b). Although this may cause the screening strength to vary locally, the observed linearity to $\Delta L$ [Fig. 3(c)] and smooth variation with $V_G$ [Fig. 4(b)] ensure that this effect is minor. Third, electrostatics shows that, at the bulk filling factor $\nu=2$, the edge of the 2DEG consists of two wide compressible strips separated by, a much narrower, incompressible strip with local filling factor $\nu=1$.[20] The data shown in this paper, which were taken at $0<G_Q<e^2/h$, should in principle correspond to the charge distribution in the outer compressible strip. However, no qualitative difference was observed when $G_Q$ was set at $e^2/h<G_Q<2e^2/h$ to detect the charge distribution in the inner compressible strip. This suggests that the EMP pulse is spread over the two compressible strips and its properties may be well characterized by the edge channel of the lowest spin-unresolved Landau level.[18]
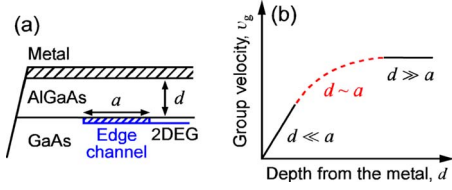
FIG. 5. (Color online) (a) Schematic cross-section of a hetero-structure covered with a metal. (b) Schematic illustration of the group velocity depending on the depth.

## IV. DISCUSSIONS

The dispersion relation and the group velocity $v_g$ of EMPs have been investigated theoretically in the long-wavelength limit for different boundary conditions. In the case of un-screened 2DEG for the etched edge,[14] the velocity $v_g$ at wave number $k$ for the fundamental EMP mode is given by

$$v_g = \frac{n_0 e}{2\pi\varepsilon B} \ln\left(\frac{e^{-C}}{2ka^*}\right), \quad (2)$$

where $\varepsilon$ is the dielectric constant of GaAs and $C$ is the form factor of the order of 1, which depends on the electron density profile around the edge channel. The $a^*$ is the characteristic width in which the EMP is mainly confined transversely to the edge channel. On the other hand, in the case of screened 2DEG with a surface metal [Fig. 5(a)],[15] $v_g$ is drastically reduced due to the screening of the in-plane electric field. When the depth of the 2DEG below the metal, $d$, is much smaller than the width of the edge channel, $a$, $v_g$ is given by

$$v_g = \frac{n_0 e}{\varepsilon B}\frac{d}{a}, \quad d \ll a. \quad (3)$$

Therefore, for the high-screening case, the velocity $v_g$ is reduced by a factor of $d/a$, which represents the degree of screening.

Figure 5(b) schematically shows how the group velocity $v_g$ depends on the screening represented by the depth $d$. In the limit of $d \ll a$, $v_g$ is reduced in proportion to the degree of screening [Eq. (3)]. In the opposite limit of $d \gg a$, the surface metal doesn't affect the EMPs and $v_g$ is expected to be independent of $d$ and approach the value given by Eq. (2). Although we do not know the analytical expression for $d \sim a$, $v_g$ is expected to vary as shown by the dashed line in Fig. 5(b). Since the surface of our device is partially covered with metallic gates, our experiment corresponds to the weak-screening regime ($d \sim a$). Therefore, the velocity $v_g$ is sensitive to the geometry of electrostatic boundary condition.

In order to evaluate the spatial profile of the edge channels in our device, we used the analytical formula given by Larkin and Davies for an edge channel induced at a depth $d$ by a semi-infinite metallic gate.[21] Fig. 6(a) shows the normalized electron density profiles, $n(x)/n_0$, for various $V_G$ at $d=110$ nm at zero magnetic field, where $n_0$ is the bulk electron density and $x$ is the lateral distance from the edge of the gate. We take for the characteristic width $a^*$ the distance between the onset of finite $n(x)$ and the half maximum, $n(x)=0.5n_0$,[14] and for the depletion length, $l$, the distance
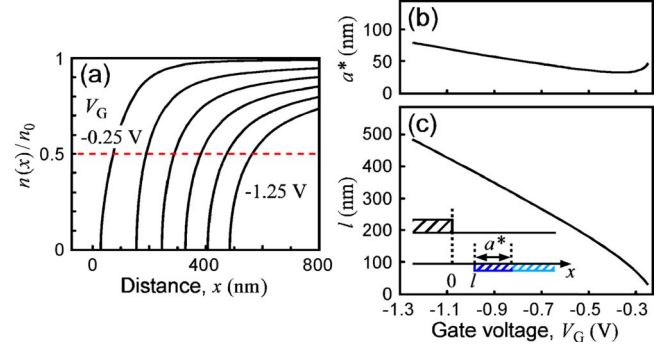


FIG. 6. (Color online) (a) Normalized electron density profiles at the distance $x$ from the gate for various $V_G$. The pinch-off voltage of $-0.2$ V and the 2DEG depth of 110 nm are used for the calculation. (b) Characteristic width $a^*$ as a function of $V_G$. (c) Depletion length $l$ as a function of $V_G$. The inset shows a schematic cross-section around the edge channel.

between the gate edge and the position of the $n(x)$ onset. They are plotted as a function of $V_G$ in Figs. 6(b) and 6(c). For sufficiently negative $V_G (< -0.3$ V), both $a^*$ and $l$ increase monotonically with decreasing $V_G$. Here, we can find two opposite effects on the velocity $v_g$. On one hand, the width $a^*$ is related to the electrostatic edge potential profile around the edge channel.[20] Eqs. (2) and (3) suggest that as $a^*$ increases, the velocity $v_g$ reduces. On the other hand, the depletion length $l$, which represents the distance between the edge channel and the metallic gate, can be regarded as the measure of screening. Analogous to the $d$ dependence of $v_g$ shown in Fig. 5(b), this implies that $v_g$ should increase as $l$ increases. The observed $V_G$ dependence indicates that the variation in the depletion length $l$ (degree of screening) has a larger effect on the velocity $v_g$ as compared to the change in the width $a^*$ (electrostatic edge potential profile).

Actually the two effects are intricately related to each other. The edge geometry ($a^*$ and $l$) is determined by the electrostatic solution for the given boundary condition.[20] Image charges induced in the gates by the EMPs affect the electrostatic edge geometry. Therefore, the velocity $v_g$ is determined self-consistently. Although quantitative discussion requires further investigation, our results clearly demonstrate that the group velocity of the EMPs has been controlled electrically by changing the degree of screening.

## V. SUMMARY

We have successfully demonstrated voltage-controlled group velocity of the EMPs in the quantum Hall regime at the bulk filling factor $\nu=2$. The group velocity strongly depends on the degree of screening caused by the metallic gate. Although we have investigated the group velocity only for $\nu=2$, we expect similar variation of the velocity for other filling factors.

Our experimental technique will be useful for conducting electronic interferometric experiments in the pulse mode as well as for studying electron dynamics in edge channels. For example, even if one of the (spin-resolved) Landau levels is selectively excited, charges in an edge channel are strongly

affected by adjacent edge channels and the injected charge is expected to be fractionalized into various edge channels.[22] Such intriguing behavior may be clarified by further investigating the local and time-resolved potential measurement developed in this work.

[1] Z. F. Ezawa, *Quantum Hall Effects: Field Theoretical Approach and Related Topics*, 2nd ed. (World Scientific, Singapore, 2008).

[2] M. Henny, S. Oberholzer, C. Strunk, T. Heinzel, K. Ensslin, M. Holland, and C. Schönenberger, Science **284**, 296 (1999).

[3] Y. Ji, Y. Chung, D. Sprinzak, M. Heiblum, D. Mahalu, and H. Shtrikman, Nature (London) **422**, 415 (2003).

[4] Y. Zhang, D. T. McClure, E. M. Levenson-Falk, C. M. Marcus, L. N. Pfeiffer, and K. W. West, Phys. Rev. B **79**, 241304(R) (2009).

[5] D. T. McClure, Y. Zhang, B. Rosenow, E. M. Levenson-Falk, C. M. Marcus, L. N. Pfeiffer, and K. W. West, Phys. Rev. Lett. **103**, 206806 (2009).

[6] N. Ofek, A. Bid, M. Heiblum, A. Stern, V. Umansky, and D. Mahalu, arXiv:0911.0794 (unpublished).

[7] I. Neder, M. Heiblum, D. Mahalu, and V. Umansky, Phys. Rev. Lett. **98**, 036803 (2007).

[8] I. Neder, N. Ofek, Y. Chung, M. Heiblum, D. Mahalu, and V. Umansky, Nature (London) **448**, 333 (2007).

[9] P. Roulleau, F. Portier, D. C. Glattli, P. Roche, A. Cavanna, G. Faini, U. Gennser, and D. Mailly, Phys. Rev. Lett. **100**, 126802 (2008).

[10] G. Fève, A. Mahé, J.-M. Berroir, T. Kontos, B. Plaçais, D. C. Glattli, A. Cavanna, B. Etienne, and Y. Jin, Science **316**, 1169 (2007).

[11] G. Fève, P. Degiovanni, and Th. Jolicoeur, Phys. Rev. B **77**, 035308 (2008).

[12] A. L. Fetter, Phys. Rev. B **32**, 7676 (1985).

[13] V. A. Volkov and S. A. Mikhailov, Zh. Eksp. Teor. Fiz. **94**, 217 (1988) [Sov. Phys. JETP **67**, 1639 (1988)].

[14] I. L. Aleiner and L. I. Glazman, Phys. Rev. Lett. **72**, 2935 (1994).

[15] M. D. Johnson and G. Vignale, Phys. Rev. B **67**, 205332 (2003).

[16] R. C. Ashoori, H. L. Stormer, L. N. Pfeiffer, K. W. Baldwin, and K. West, Phys. Rev. B **45**, 3894 (1992).

[17] G. Ernst, R. J. Haug, J. Kuhl, K. von Klitzing, and K. Eberl, Phys. Rev. Lett. **77**, 4245 (1996).

[18] G. Sukhodub, F. Hohls, and R. J. Haug, Phys. Rev. Lett. **93**, 196801 (2004).

[19] H. Kamata, T. Ota, and T. Fujisawa, Jpn. J. Appl. Phys. **48**, 04C149 (2009).

[20] D. B. Chklovskii, B. I. Shklovskii, and L. I. Glazman, Phys. Rev. B **46**, 4026 (1992).

[21] I. A. Larkin and J. H. Davies, Phys. Rev. B **52**, R5535 (1995).

[22] E. Berg, Y. Oreg, E.-A. Kim, and F. von Oppen, Phys. Rev. Lett. **102**, 236402 (2009).